

# Improving the Performance of Lithium–Sulfur Batteries by Conductive Polymer Coating

Yuan Yang,<sup>†,§</sup> Guihua Yu,<sup>‡,§</sup> Judy J. Cha,<sup>†</sup> Hui Wu,<sup>†</sup> Michael Vosgueritchian,<sup>‡</sup> Yan Yao,<sup>†</sup> Zhenan Bao,<sup>‡,\*</sup> and Yi Cui<sup>†,⊥,\*</sup>

<sup>†</sup>Department of Materials Science and Engineering, and <sup>‡</sup>Department of Chemical Engineering, Stanford University, Stanford, California 94305, United States and, <sup>⊥</sup>SLAC National Accelerator Laboratory, Stanford Institute for Materials and Energy Sciences, 2575 Sand Hill Road, Menlo Park, California 94025, United States.

<sup>§</sup>These authors contributed equally to this paper.

Rechargeable batteries with high specific energy are important for portable electronic devices, power tools, and electric vehicles.<sup>1–3</sup> Though Li ion batteries have the highest specific energy among rechargeable batteries, they still do not meet energy requirements for many applications, such as vehicle electrification.<sup>4,5</sup> Novel materials and designs are desired to realize batteries with higher specific energy.<sup>6–10</sup> The relatively low capacity of cathodes is one of the limiting factors for achieving battery cells with high specific energy. Current cathode materials, such as transition metal oxides and phosphates, have an inherent limit of  $\sim 300$  mAh/g.<sup>11</sup> On the other hand, sulfur cathodes have a theoretical capacity of 1673 mAh/g. Though its voltage is 2.2 V vs Li/Li<sup>+</sup>, the theoretical specific energy of the Li/S cell is  $\sim 2600$  Wh/kg, 5 times higher than the commercialized Li-CoO<sub>2</sub>/graphite system.<sup>12,13</sup> Sulfur as a cathode material also has other advantages such as low cost and nontoxicity. However, the poor cycle life of Li/S batteries is a significant barrier toward its commercialization.<sup>14–17</sup> There are a number of reasons leading to the fast capacity fading, including the dissolution of intermediate lithium polysulfide products (Li<sub>2</sub>S<sub>*x*</sub>, 4 ≤ *x* ≤ 8) in the electrolyte,<sup>16</sup> the large volumetric expansion of sulfur ( $\sim 80\%$ ) during cycling, and the insulating nature of Li<sub>2</sub>S. Mesoporous carbon has been reported to be effective at trapping polysulfides due to their small pore diameter.<sup>11,18</sup> Nevertheless, there is still a large surface area for polysulfides to escape, as the particle size of the mesoporous carbon matrix is only 0.5–1 μm (Figure 1a). As a result, a capacity decay of  $\sim 10\%$  for the first 20 cycles was observed in mesoporous carbon/sulfur composite. To tackle this issue, a

polyethylene oxide (PEO) layer was linked on the surface of mesoporous carbon to trap polysulfides.<sup>11</sup> Though the discharge capacity was improved, the cycling performance remained similar to cells without the PEO layer. This is likely due to the fact that a monolayer of polymer is not enough to fully trap polysulfides. In order to confine polysulfides more effectively, the surface coating layer should be rigid and stable, but not too rigid to break during the expansion of sulfur upon cycling. Moreover, it needs to be both ionically and electronically conductive, as illustrated in Figure 1. Poly(3,4-ethylenedioxythiophene)-poly(styrene sulfonate) (PEDOT:PSS) is a good choice based on these criteria, as it is stable and moderately rigid in the electrochemical environment.<sup>19,20</sup> PEDOT:PSS is also reported to be thermally stable at 85 °C for over 1000 h with minimal change on electrical conductivity.<sup>21</sup> Herein we explore the unique application of PEDOT:PSS-based conductive polymer for further improving the electrode performance of CMK-3 mesoporous carbon/sulfur composite. With the assistance of PEDOT:PSS coating, the capacity retention of sulfur electrode is enhanced from  $\sim 70\%/100$  cycles to  $\sim 80\%/100$  cycles with 10% increase in delivered discharge capacity. Especially after 80 cycles, the capacity decay is only 15%/100 cycles with polymer coating, while the bare counterpart exhibits a capacity decay of 40%/100 cycles. The coulomb efficiency is also significantly improved from 93% to 97%.

## RESULTS AND DISCUSSION

CMK-3 mesoporous carbon was used in this study as a model system.<sup>11</sup> The porous carbon was synthesized according to an

\* Address correspondence to yicui@stanford.edu; zbao@stanford.edu.

Received for review September 6, 2011 and accepted October 13, 2011.

Published online October 13, 2011  
10.1021/nn203436j

© 2011 American Chemical Society

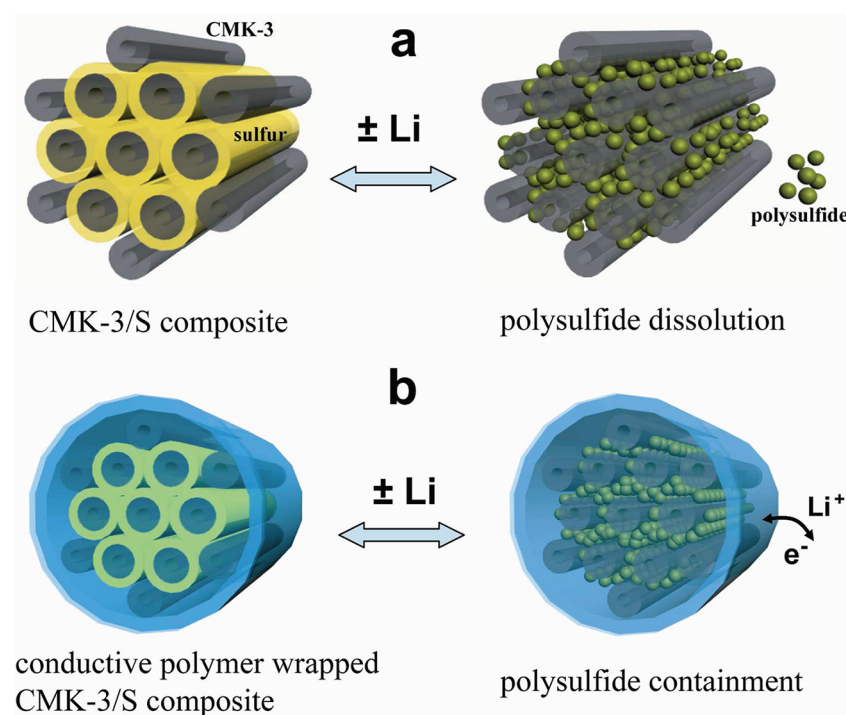


**Figure 1.** Scheme of PEDOT:PSS-coated CMK-3/sulfur composite for improving the cathode performance. (a) In bare CMK-3/S particles (gray: CMK-3, yellow: sulfur), polysulfides (green color) still diffuse out of the carbon matrix during lithiation/delithiation. (b) With conductive polymer coating layer (blue color), polysulfides could be confined within the carbon matrix. Lithium ions and electrons can move through this polymer layer.

established approach.<sup>22</sup> The Brunauer–Emmet–Teller (BET) measurement showed that the as-synthesized particles had a surface area of 1100–1200 m<sup>2</sup>/g and pore volume of 1–1.1 cm<sup>3</sup>/g. Sulfur was loaded into the mesoporous carbon by heating a mixture of the CMK-3 carbon and sulfur at a weight ratio of 1:1. Polymer coating was achieved by dispersing and sonicating CMK-3/sulfur particles in a 0.08 wt % PEDOT:PSS solution for 1 h (see Methods section). Figure 2a and b show scanning electron microscope (SEM) images of bare and PEDOT:PSS-coated CMK-3/sulfur composite, respectively. The particle size of these two kinds of samples is similar, about 0.5–1 μm. However, it is obvious that the surface looks different. In Figure 2b, the CMK-3/sulfur particles are wrapped by a polymer layer and the surface appears smoother. Polymer is also found between particles, as indicated by the arrows. The polymer between particles acts as a binder to improve the adhesion between particles and between particles and aluminum substrate. The as-made electrode sticks to the aluminum substrate very well.

X-ray photoelectron spectroscopy (XPS) was used to further confirm and characterize the polymer coating layer on the surface of the sulfur electrode. Figure 3a–c show the sulfur (2p) peak of pure PEDOT:PSS film, CMK-3/sulfur composite, and PEDOT:PSS-coated CMK-3/sulfur from top to bottom. Pure PEDOT:PSS film exhibits two peaks, at 168.0 and 163.6 eV, respectively. Further fitting indicates that each peak can be split into two peaks. The two with higher energies of 168.7 and

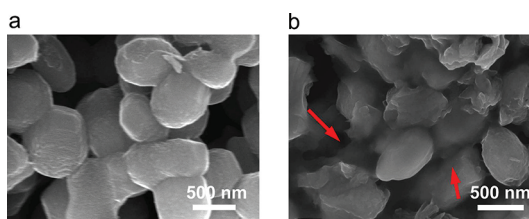


**Figure 2.** SEM images of CMK-3/sulfur particles before (a) and after (b) PEDOT:PSS coating. In the sample with polymer coating, the particles were wrapped by a polymer layer. The arrows indicate PEDOT:PSS polymer between particles.

167.5 eV can be assigned to poly(styrene sulfonate), and the other two at 165.3 and 163.5 eV are attributed to PEDOT.<sup>23</sup> CMK-3/sulfur shows two peaks, at 163.2 and 164.3 eV, which are the characteristic peaks of elemental sulfur. A weak broad peak centered between 169 and 170 eV is observed, which is likely due to the surface oxidation of sulfur or strong interaction between sulfur and mesoporous carbon.<sup>24</sup> The PEDOT:PSS-coated CMK-3/sulfur sample shows an XPS spectrum very similar to that of pure PEDOT:PSS film. The peak at 168 eV could be assigned to PSS. This proves that PEDOT:PSS is present on the surface of CMK-3/sulfur particles. As the positions of PEDOT and CMK-3/sulfur peaks are too close to each other, it is hard to separate the contribution of PEDOT and CMK-3/sulfur to the peak at 164 eV. However, as the intensity ratio of the two broad peaks is close to that of pure PEDOT:PSS film, it is likely that most signals come from

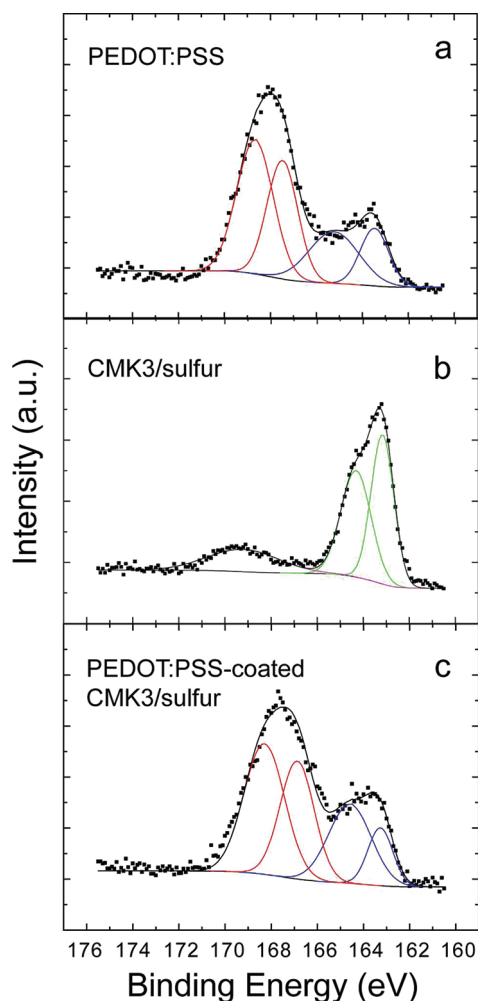


Figure 3. XPS characterization of PEDOT:PSS-coated CMK-3/sulfur particles. From top to bottom: (a) pure PEDOT:PSS film, (b) bare CMK-3/sulfur particles, and (c) PEDOT:PSS-coated CMK-3/sulfur particles.

PEDOT, not elemental sulfur. Furthermore, as the penetration depth of XPS is about 10 nm, it is likely that the possible elemental sulfur signal comes from places where the polymer layer is thinner than 10 nm. The SEM and XPS results indicate that most of the surface area of the particles is covered with PEDOT:PSS polymer; thus the coating is quite conformal.

Transmission electron microscope (TEM) was further used to examine the morphology and property of the PEDOT:PSS coating on individual CMK-3/sulfur particles. Figure 4a exhibits a bright field TEM image of agglomerated particles coated with PEDOT:PSS. The particle size is close to 1  $\mu\text{m}$ . Figure 4b shows a zoom-in image of the region marked by the red rectangle in Figure 4a. In this figure, vague parallel lines can be observed in the particle, which reflects the hexagonal packing structure of carbon tubes in the CMK-3 mesoporous carbon.<sup>11</sup> The lines are not as clear as those in bare CMK-3/sulfur particles (Figure S1) due to the polymer coating. We observed that these lines did not extend to the edge of particles, but they were surrounded by a thin, amorphous

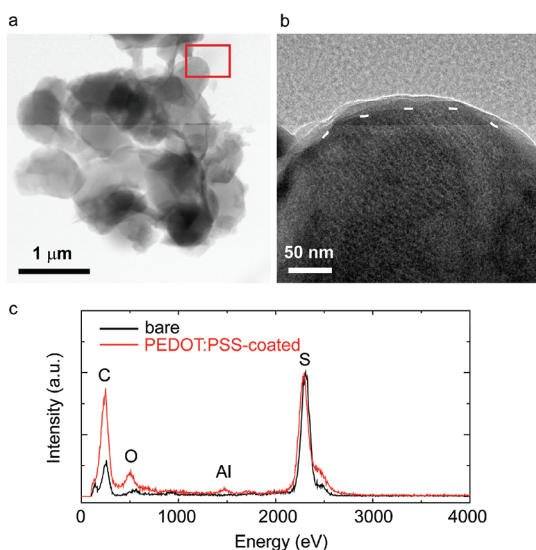
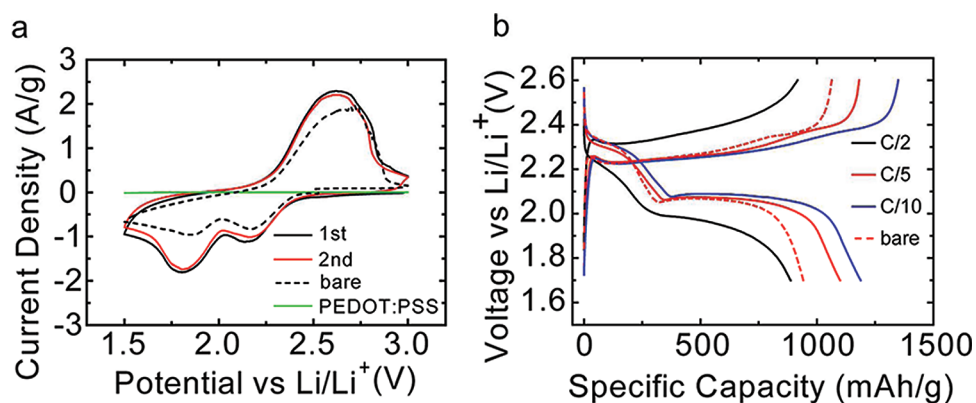


Figure 4. (a) Bright field TEM image of PEDOT:PSS-coated CMK-3/sulfur particles at low magnification. (b) Zoom-in TEM image of the region marked by the red rectangle in (a). The boundary between mesoporous carbon particle and polymer coating is guided by the dashed line. (c) EDS spectra of PEDOT:PSS-coated (red) and bare (black) CMK-3/sulfur particles. The two spectra are normalized to the sulfur peak.

TABLE 1. Weight Percentage of Elements in PEDOT:PSS Polymer and CMK-3/Sulfur Composite, Respectively

	C	S	O	H
PEDOT:PSS	52	19	25	4
CMK-3/sulfur	50	50	0	0

layer with a thickness of  $\sim 10$  nm, as guided by the dashed line. Such an amorphous layer has been observed on most particles (Figure S2 shows additional particles with surface coating layer), and the thickness was typically 10–20 nm. This is obviously different from TEM images of their bare counterpart. In bare CMK-3/sulfur samples, the parallel lines clearly reach the edge of particles and no coating is observed (Figure S1). The contrast between the coating layer and CMK-3/sulfur particle is not strong, which could be explained by the similar elemental composition of PEDOT and CMK-3/sulfur. As shown in Table 1, PEDOT:PSS and CMK-3/sulfur composite contain almost the same amount of carbon in weight (52% vs 50%), although PEDOT:PSS has less sulfur element (19% vs 50%) and contains more oxygen (25%) and hydrogen (4%). Consequently, the coating layer appears lighter under the bright field TEM, but no significant contrast could be observed. Corresponding energy-dispersive X-ray spectroscopy (EDS) of polymer-coated and bare CMK-3/sulfur particles is illustrated in Figure 4c. The two spectra are normalized to the sulfur peak. In the bare sample, the relative intensity of the carbon peak is remarkably lower, as the portion of carbon in bare CMK-3/sulfur is much less compared to the PEDOT:PSS-coated



**Figure 5.** Electrochemical characterization of PEDOT:PSS-coated CMK-3/sulfur particles. (a) Cyclic voltammetry of PEDOT:PSS-coated CMK-3/sulfur particles in the first two cycles and pure PEDOT:PSS film. (b) Voltage profiles of PEDOT:PSS-coated CMK-3/sulfur particles at different current rates (1C = 1673 mA/g). The second charge/discharge curves are presented in the plot.

sample (Table 1). Moreover, though a trace amount of oxygen is detected in bare particles due to surface oxidation and silica residue, the spectrum of polymer-coated CMK-3/sulfur shows a significantly higher peak of oxygen at 0.51 keV. Since oxygen exists only in PEDOT:PSS, but not in CMK-3/sulfur composite, this further proves that the amorphous layer is PEDOT:PSS. A trace amount of Al was detected too. This is due to the acidity of the PEDOT:PSS solution, which leads to a small amount of dissolution of Al substrate. However, no effect on the electrochemical performance has been observed, as discussed later. On the basis of results from SEM, XPS, and TEM, we believe that PEDOT:PSS conductive polymer coating on the CMK-3/sulfur particles is achieved by the simple sonication approach.

To study the electrochemical characteristics of PEDOT:PSS-coated CMK-3/sulfur composites, cyclic voltammetry (CV) was first performed at a scan speed of 0.2 mV/s (Figure 5a). The PEDOT:PSS-coated CMK-3/sulfur sample exhibited the same characteristics as the sulfur electrode. Under cathodic current, two reductive peaks at 2.15 and 1.80 V were observed, corresponding to the redox reaction of high-order polysulfides and  $\text{Li}_2\text{S}_2/\text{Li}_2\text{S}$ , respectively. When the voltage sweep was reversed, the CV plot exhibited a broad peak at 2.63 V with a shoulder at 2.80 V. This indicates that two oxidative peaks exist and overlap with each other, which corresponds to the reverse reactions. We also carried out a CV scan at a lower scan rate of 0.1 mV/s. In this case, the redox peaks are closer to the equilibrium potential of the corresponding reaction (Figure S3), as the positions of peaks are scan rate-dependent. Little difference is observed between the first and the second scan, suggesting a subtle decay in capacity upon cycling. The CV profile of the bare CMK-3/sulfur sample is presented as a dashed line. The redox peaks exist at similar positions, but their amplitudes are smaller. The CV scan result of pure PEDOT:PSS film is also presented by the blue curve. The absolute magnitude of the current is two orders smaller than that of

the PEDOT:PSS-coated CMK-3/sulfur electrode; thus the contribution of PEDOT:PSS to the capacity is negligible.

The voltage profiles of polymer-coated CMK-3/sulfur composites at different current rates are shown in Figure 5b. Consistent with results from cyclic voltammetry, we observed the typical two-plateau behavior of the sulfur cathode, corresponding to the formation of long-chain polysulfides ( $\text{Li}_2\text{S}_x$ ,  $4 \leq x \leq 8$ ) at 2.3 V and short-chain  $\text{Li}_2\text{S}_2$  and  $\text{Li}_2\text{S}$  at 2.1 V. The discharge capacity of the second discharge cycle was 1179 mAh/g at a current rate of C/10 (1C = 1673 mA/g), which is much higher than the bare mesoporous/sulfur composite.<sup>11,25</sup> The discharge capacity remained as high as 1092 and 885 mAh/g at C/5 and C/2, respectively. To separate the contribution of PEDOT:PSS and sulfur to the overall capacity, the electrochemical characteristics of PEDOT:PSS film were examined at a current rate of 100 mA/g, as shown in Figure S4. Capacity of less than 1.0 mAh/g can be extracted from PEDOT:PSS itself. This means that PEDOT:PSS used in our experiment was not involved in any noticeable electrochemical reaction in the voltage window of sulfur electrode (1.7–2.6 V vs  $\text{Li/Li}^+$ ). The voltage profile of bare CMK-3/sulfur particles is shown by the red dashed line in Figure 5b. The discharge capacity is 941 mAh/g, which is 14% less than that of polymer-coated CMK-3/sulfur. There are two possible reasons. First, the PEDOT:PSS coating help trap polysulfides so that more polysulfides could be converted to  $\text{Li}_2\text{S}$ . This is supported by the fact that the major difference in capacity comes from the second discharge plateau. The other possible reason is that the high electronic conductivity of PEDOT:PSS<sup>26</sup> as a conductive coating is capable of enhancing the rate performance of insulating materials.<sup>20,27–29</sup>

The cycling performance of the PEDOT:PSS-coated CMK-3/sulfur cathode is shown in Figure 6a, together with that of the bare CMK-3/sulfur cathode. The current rate is C/5 (1C = 1673 mA/g). The initial discharge capacity was 1051 mAh/g for bare CMK-3/sulfur

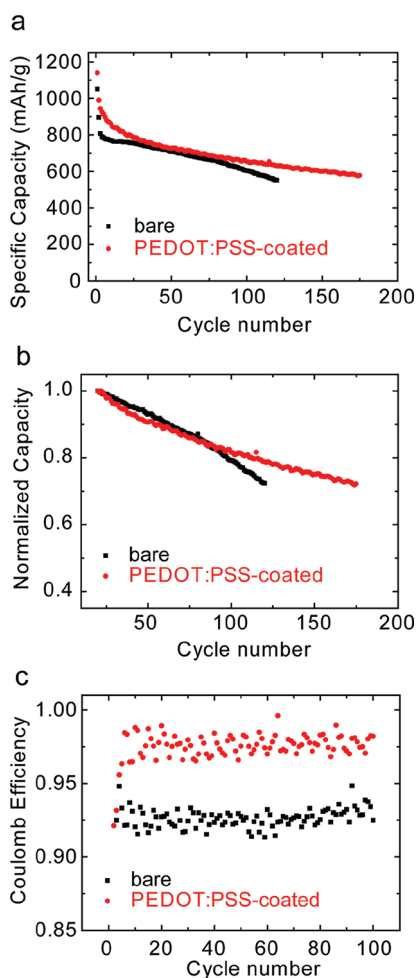


**Figure 6.** Performance comparison of PEDOT:PSS-coated and bare CMK-3/sulfur particles as cathode materials. (a) Absolute discharge capacity and (b) normalized discharge capacity against cycle number. The decay accelerated in bare samples, while it slowed down in polymer-coated ones. (c) Coulomb efficiency comparison of both polymer-coated and bare samples in the first 100 cycles.

particles, while the polymer-coated sample delivered a discharge capacity of 1140 mAh/g, which is 9% higher than that of the bare counterpart. In the bare sample, the discharge capacity stabilized around 730 mAh/g between the fifth and 20th cycles, and the capacity decay was as low as 0.1% per cycle during these cycles. However, after 20 cycles, the capacity decay rate increased to 0.29% per cycle in the following 100 cycles. It is likely that polysulfides can be trapped in pores of mesoporous carbon for a short time, such as several days. However, as no real capping layer exists, polysulfides can still diffuse out upon a prolonged span of time. In contrast, the PEDOT:PSS-coated CMK-3/sulfur composite showed slightly faster decay at the beginning, but the discharge capacity stabilized after 20 cycles. The discharge capacity at the 20th cycle reached 801 mAh/g for conductive polymer-coated samples. After that, a decay rate of only 0.21% per cycle was observed in the following 100 cycles. The capacity

remained over 600 mAh/g even after 150 cycles. This suggests that polysulfides are better trapped inside the carbon matrix due to the polymer coating on the surface of the CMK-3/sulfur composite. To better compare the cycling performance of polymer-coated and bare CMK-3/sulfur particles, the discharge capacity is normalized to that at the 20th cycles (Figure 6b). It is obvious that polymer-coated samples showed a superior cycling performance in the long run. Especially between the 80th and 120th cycles, the bare CMK-3/sulfur sample exhibited a capacity decay of 40% per 100 cycles, while the PEDOT:PSS-coated counterpart decayed as little as 15% per 100 cycles. This further proves that the decay accelerated in bare samples but slowed down in those with a protective polymer coating. There are two possible reasons accounting for the remaining decay of 0.2% per cycle. First, small amounts of particles were not conformally coated with the polymer so that a leakage path for polysulfide dissolution still exists. Second, the volume expansion and contraction of the sulfur electrode might lead to the degradation of the PEDOT coating layer under mechanical strain. Optimization of the polymer concentration and selection of polymer in the future could further minimize the polysulfide leakage and the polymer coating fatigue. We notice that recently there is a report on using commercial PEDOT:PSS binder to improve the performance of mesoporous carbon/sulfur composite, which shows a capacity decay of 20–25%/100 cycles at a 0.1 C rate.<sup>30</sup> The results are consistent with our observations.

The better trapping capability of the PEDOT:PSS coating is also reflected in the improved coulomb efficiency (Figure 6c). In bare samples, the coulomb efficiency of the sulfur electrode was about 92–94%. After polymer coating, the coulomb efficiency increased to 96–98% at the same current rate. It was reported that 99.84% coulomb efficiency was achieved based on the bare CMK-3/sulfur sample.<sup>11</sup> However, data of only one cycle were presented. In our work, we notice that it was possible to achieve coulomb efficiency between 99% and 101% in the first several cycles due to a competition between shuttle effect and capacity decay during charging. However, it has never been observed that coulomb efficiency could reach over 99% for more than several cycles. In addition, both cycling and coulomb efficiency showed small fluctuations with a periodicity of one day, which should be induced by variation of the environmental temperature.

To further understand the effect of PEDOT:PSS coating on transport characteristics of the sulfur electrode, electrochemical impedance spectroscopy (EIS) is performed on both polymer-coated and bare CMK-3/sulfur electrodes (Figure S5). Three different states are examined, including before discharging, the end of the first discharge, and the end of the first charge, as shown in Figure S5b–d. All impedance results show

depressive semicircles. At the beginning, the charge transfer resistance of the PEDOT:PSS-coated sample is smaller than that of bare CMK-3/sulfur particles. However, at the end of discharge, the impedance of the polymer-coated sample increases to be slightly larger than that of bare CMK-3/sulfur particles, and there is likely a second semicircle in the PEDOT:PSS-coated sample. This is possibly due to a lithiated PEDOT layer, which slightly impedes the charge transfer and at the same time blocks polysulfide diffusion. After charging back, the impedance of PEDOT:PSS-coated and bare particles becomes close to each other. These impedance results indicate that the PEDOT:PSS coating layer can transport lithium ions and electrons readily, though a small kinetic barrier may exist due to the polymer layer. However, this barrier does not lead to lower capacity or poorer cycle life. This means that the specific capacity and cycle life are dominated by polysulfide diffusion and volume expansion of sulfur.

## METHODS

**Synthesis of Mesoporous Carbon/Sulfur Composite.** The composite was prepared as described in previous papers.<sup>11,22</sup> First, SBA-15 mesoporous silica was synthesized as a template for CMK-3 porous carbon. The mesoporous silica was made by hydrolysis of tetraethylorthosilicate under acidic condition with the help of Pluronic P123 (EO20PPO70EO20). To create CMK-3 mesoporous carbon, 0.5 g of SBA-15 was dispersed and sonicated in 2.5 mL of water with 0.625 g of sucrose and 0.07 g of H<sub>2</sub>SO<sub>4</sub> dissolved inside. Then the mixture was heated at 100 °C for 6 h, followed by another 6 h at 160 °C. This sucrose infiltration process was then repeated with a 2.5 mL aqueous solution containing 0.4 g of sucrose and 45 mg of H<sub>2</sub>SO<sub>4</sub>. Finally, the composite was carbonized at 900 °C in a nitrogen atmosphere, and silica template was removed by 5% HF solution. Infiltration of sulfur into CMK-3 porous carbon was achieved by heating well-mixed CMK-3/sulfur at 155 °C for 12 h. The weight ratio of carbon to sulfur was 1:1.

**Preparation of PEDOT:PSS-Coated CMK-3/Sulfur Composite.** Poly(3,4-ethylenedioxythiophene)/poly(styrene sulfonate) (PEDOT:PSS) solution was prepared by filtering commercially available solution (~1 wt % solid content, Clevis PH1000) and adding 5% dimethyl sulfoxide (DMSO), and subsequently diluted with deionized water at volume ratio of 1:10 (~0.1 wt %). A 25 wt % of extra ethanol was added to improve the wetting between CMK-3/sulfur particles and the polymer solution (final PEDOT:PSS concentration is ~0.08 wt %). To coat PEDOT:PSS onto CMK-3/sulfur composites, 10 mg of CMK-3/sulfur composite particles was added into 1 mL of as-prepared PEDOT:PSS solution and bath sonicated for 1 h.

**Electrode Fabrication and Electrochemical Measurement.** The sulfur electrode was made by drop casting the solution onto aluminum foil and drying at 60 °C under vacuum. Then the sample was baked at 80 °C for another 30 min. No binder or extra conductive additive was used. Control samples without PEDOT:PSS coating were prepared in the same way. 2032-type coin cells were fabricated for electrochemical testing. Lithium was used as the counter electrode. The electrolyte was 1 M lithium bis(trifluoromethanesulfonyl)imide (LiTFSI) in 1,3-dioxolane and 1,2-dimethoxyethane (volume ratio 1:1). The typical mass loading of cathode materials was 1.0 mg/cm<sup>2</sup>, and the percentage of sulfur in the electrode is ~43%. Impedance spectroscopy and cyclic voltammetry results were measured by a coin cell-based three-electrode configuration with lithium as both the counter electrode and the reference electrode.<sup>31</sup> The frequency range for impedance study was 200 kHz to 0.1 Hz.

In summary, we have demonstrated that conductive polymer PEDOT:PSS coating on the surface of mesoporous carbon/sulfur particles could be used to effectively trap polysulfides and minimize the dissolution of polysulfides and the loss of active mass in cathodes, which leads to a notable improvement of the performance of Li–S batteries. The initial discharge capacity reached 1140 mAh/g, which is ~10% higher than that of the bare counterpart. More significantly, the discharge capacity remained over 600 mAh/g at the 150th cycle. The cycle life and coulomb efficiency were markedly improved. In prolonged cycling, the capacity retention increased from ~60%/100 cycles to ~85%/100 cycles. Coulomb efficiency also increased from 93% to 97%. The strategy of conductive polymer coating on the exterior surface of active electrodes can be potentially generalized for improving the performance of other electrode materials in lithium ion batteries.

**Acknowledgment.** Y.Y. acknowledges support from a Stanford Graduate Fellowship. Y.C. and Z.B. acknowledge the funding support from the Precourt Institute for Energy at Stanford University. Y.C. also acknowledges the funding support from the King Abdullah University of Science and Technology (KAUST) Investigator Award (No. KUS-I1-001-12). A portion of this work was supported by the Department of Energy, Office of Basic Energy Sciences, Division of Materials Sciences and Engineering, under contract DE-AC02-76SF00515 through the SLAC National Accelerator Laboratory LDRD project.

**Supporting Information Available:** Additional experimental details and figures are available free of charge via the Internet at <http://pubs.acs.org>.

## REFERENCES AND NOTES

1. Tarascon, J. M.; Armand, M. Issues and Challenges Facing Rechargeable Lithium Batteries. *Nature* **2001**, *414*, 359–367.
2. Arico, A. S.; Bruce, P.; Scrosati, B.; Tarascon, J. M.; Van Schalkwijk, W. Nanostructured Materials for Advanced Energy Conversion and Storage Devices. *Nat. Mater.* **2005**, *4*, 366–377.
3. Whittingham, M. S. Lithium Batteries and Cathode Materials. *Chem. Rev.* **2004**, *104*, 4271–4301.
4. Kang, B.; Ceder, G. Battery Materials for Ultrafast Charging and Discharging. *Nature* **2009**, *458*, 190–193.
5. Chung, S. Y.; Bloking, J. T.; Chiang, Y. M. Electronically Conductive Phospho-Olivines as Lithium Storage Electrodes. *Nat. Mater.* **2002**, *1*, 123–128.
6. Manthiram, A.; Murugan, A. V.; Sarkar, A.; Muraliganth, T. Nanostructured Electrode Materials for Electrochemical Energy Storage and Conversion. *Energy Environ. Sci.* **2008**, *1*, 621–638.
7. Chan, C. K.; Peng, H. L.; Liu, G.; McIlwrath, K.; Zhang, X. F.; Huggins, R. A.; Cui, Y. High-Performance Lithium Battery Anodes Using Silicon Nanowires. *Nat. Nanotechnol.* **2008**, *3*, 31–35.
8. Wang, H. L.; Yang, Y.; Liang, Y. Y.; Cui, L. F.; Casaloungue, H. S.; Li, Y. G.; Hong, G. S.; Dai, H. J.; Cui, Y. LiMn<sub>1-x</sub>Fe<sub>x</sub>PO<sub>4</sub> Nanorods Grown on Graphene Sheets for Ultrahigh-Rate-Performance Lithium Ion Batteries. *Angew. Chem., Int. Ed.* **2011**, *50*, 7364–7368.
9. Hu, L. B.; Choi, J. W.; Yang, Y.; Jeong, S.; La Mantia, F.; Cui, L. F.; Cui, Y. Highly Conductive Paper for Energy-Storage

- Devices. *Proc. Natl. Acad. Sci. U. S. A.* **2009**, *106*, 21490–21494.
10. Duduta, M.; Ho, B.; Wood, V. C.; Limthongkul, P.; Brunini, V. E.; Carter, W. C.; Chiang, Y.-M. Semi-Solid Lithium Rechargeable Flow Battery. *Adv. Energy Mater.* **2011**, *1*, 511–516.
11. Ji, X. L.; Lee, K. T.; Nazar, L. F. A Highly Ordered Nanostructured Carbon-Sulphur Cathode for Lithium-Sulphur Batteries. *Nat. Mater.* **2009**, *8*, 500–506.
12. Joongpyo, S.; Striebel, K. A.; Cairns, E. J. The Lithium/Sulfur Rechargeable Cell. *J. Electrochem. Soc.* **2002**, *149*, A1321–5.
13. Wang, H. L.; Yang, Y.; Liang, Y. Y.; Robinson, J. T.; Li, Y. G.; Jackson, A.; Dai, H. J.; Cui, Y. Graphene-Wrapped Sulfur Particles as a Rechargeable Lithium-Sulfur Battery Cathode Material with High Capacity and Cycling Stability. *Nano Lett.* **2011**, *11*, 2644–2647.
14. Yamin, H.; Gorenstein, A.; Penciner, J.; Sternberg, Y.; Peled, E. Lithium Sulfur Battery - Oxidation Reduction-Mechanisms of Polysulfides in THF Solutions. *J. Electrochem. Soc.* **1988**, *135*, 1045–1048.
15. Lee, Y. M.; Choi, N. S.; Park, J. H.; Park, J. K. Electrochemical Performance of Lithium/Sulfur Batteries with Protected Li Anodes. *J. Power Sources* **2003**, *119*, 964–972.
16. Mikhaylik, Y. V.; Akridge, J. R. Polysulfide Shuttle Study in the Li/S Battery System. *J. Electrochem. Soc.* **2004**, *151*, A1969–A1976.
17. Zheng, W.; Liu, Y. W.; Hu, X. G.; Zhang, C. F. Novel Nanosized Adsorbing Sulfur Composite Cathode Materials for the Advanced Secondary Lithium Batteries. *Electrochim. Acta* **2006**, *51*, 1330–1335.
18. Liang, C. D.; Dudney, N. J.; Howe, J. Y. Hierarchically Structured Sulfur/Carbon Nanocomposite Material for High-Energy Lithium Battery. *Chem. Mater.* **2009**, *21*, 4724–4730.
19. Zhan, C. M.; Zhan, L. Z.; Song, Z. P.; Zhang, J. Y.; Tang, J.; Zhan, H.; Zhou, Y. H. PEDOT: Cathode Active Material with High Specific Capacity in Novel Electrolyte System. *Electrochim. Acta* **2008**, *53*, 8319–8323.
20. Murugan, A. V.; Muraliganth, T.; Manthiram, A. Rapid Microwave-solvothermal Synthesis of Phospho-olivine Nanorods and Their Coating with a Mixed Conducting Polymer for Lithium Ion Batteries. *Electrochem. Commun.* **2008**, *10*, 903–906.
21. Elschner, A.; Kirchmeyer, S.; Lovenich, W.; Merker, U.; Reuter, K. *PEDOT: Principles and Applications of an Intrinsically Conductive Polymer*; CRC Press: Boca Raton, FL, USA, 2010.
22. Yang, Y.; McDowell, M. T.; Jackson, A.; Cha, J. J.; Hong, S. S.; Cui, Y. New Nanostructured Li<sub>2</sub>S/Silicon Rechargeable Battery with High Specific Energy. *Nano Lett.* **2010**, *10*, 1486–1491.
23. Greczynski, G.; Kugler, T.; Salaneck, W. R. Characterization of the PEDOT-PSS System by Means of X-ray and Ultraviolet Photoelectron Spectroscopy. *Thin Solid Films* **1999**, *354*, 129–135.
24. Toniazzo, V.; Mustin, C.; Portal, J. M.; Humbert, B.; Benoit, R.; Erre, R. Elemental Sulfur at the Pyrite Surfaces: Speciation and Quantification. *Appl. Surf. Sci.* **1999**, *143*, 229–237.
25. Ji, X. L.; Evers, S.; Black, R.; Nazar, L. F. Stabilizing Lithium-Sulphur Cathodes Using Polysulphide Reservoirs. *Nat. Commun.* **2011**, *2*, 325.
26. Groenendaal, B. L.; Jonas, F.; Freitag, D.; Pielartzik, H.; Reynolds, J. R. Poly(3,4-ethylenedioxythiophene) and its Derivatives: Past, Present, and Future. *Adv. Mater.* **2000**, *12*, 481–494.
27. Wang, Y.; Cao, G. Z. Developments in Nanostructured Cathode Materials for High-Performance Lithium-Ion Batteries. *Adv. Mater.* **2008**, *20*, 2251–2269.
28. Yamada, A.; Hosoya, M.; Chung, S. C.; Kudo, Y.; Hinokuma, K.; Liu, K. Y.; Nishi, Y. Olivine-Type Cathodes Achievements and Problems. *J. Power Sources* **2003**, *119*, 232–238.
29. Chen, Z. H.; Dahn, J. R. Reducing Carbon in LiFePO<sub>4</sub>/C Composite Electrodes to Maximize Specific Energy, Volumetric Energy, and Tap Density. *J. Electrochem. Soc.* **2002**, *149*, A1184–A1189.
30. Li, X. L.; Cao, Y. L.; Qi, W.; Saraf, L. V.; Xiao, J.; Nie, Z. M.; Mietek, J.; Zhang, J. G.; Schwenzer, B.; Liu, J. Optimization of Mesoporous Carbon Structures for Lithium-Sulfur Battery Applications. *J. Mater. Chem.* **2011**, *21*, 16603–16610.
31. Barchasz, C.; Lepretre, J.-C.; Alloin, F.; Patoux, S. New Insights into the Limiting Parameters of the Li/S Rechargeable Cell. *J. Power Sources* **2011**, doi: 10.1016/j.jpowsour.2011.07.021.